125. The Structure of an Isomeric Pair of a (Tetraamine)copper(II) Compound in the Solid State and in Solution

by **Peter Comba***, **Peter Hilfenhaus**, and **Bernhard Nuber**

Anorganisch-Chemisches Institut der Universität, Im Neuenheimer Feld 270, 69120 Heidelberg

Dedicated to Professor *Achim Müller* on the occasion of his 60th birthday

(1.IV.97)

The template condensation of $[Cu(3,2,3\text{-tet})]^{2+}$ (3,2,3-tet = *N*,*N*''-(ethane-1,2-diyl)propane-1,3-diamine with CH_2O and en (en = ethane-1,2-diamine) affords the copper(II) compounds of two isomeric tricyclic ligands in high yield. The strikingly different UV/VIS and EPR spectroscopic behavior of these two compounds, [Cu('*syn*'-L)]$(ClO_4)_2$ and [Cu('*anti*'-L)]$(ClO_4)_2 \cdot \frac{1}{2}H_2O$ (L = 1,4,8,10,13,15-hexaazatricyclo [13.3.1.1^{4,8}]icosane), is analyzed by angular overlap model (AOM) calculations based on the experimentally determined solid-state structures (powder spectra) and a combination of molecular mechanics and AOM calculations (MM-AOM) for the solution-structure behavior.

1. Introduction. – It is not uncommon that an experimentally determined structure, obtained by the analysis of X-ray diffraction data from crystals, is not directly related to the structure of the species in solution. This is a particular problem for coordination compounds of labile metal ions. For example, or [Cu^{II}(tetraamines)] with constant amine ligands, coordination numbers (4, 5, or 6), coordination geometries (distortion of the square-planar arrangement of the equatorial ligands), and the axial donor groups (anion or solvent) are frequently different in the solid and in solution. Consequently, the colors and other properties may differ dramatically. Spectroscopy is an important tool to analyze the structural properties in solution. We have developed methods based on the combination of force-field (MM) and ligand-field (angular-overlap model, AOM) calculations, to obtain structural information of transition-metal compounds in solution (MM-AOM) [1]. The assignment of the ligand-field transitions and the interpretation of the electronic and EPR spectra of [Cu^{II}(tetraamine)] complexes, and the parametrization of the corresponding force-field potentials and of the AOM matrices, have been thoroughly tested, based on a series of [Cu^{II}(tetraamine)] complexes, involving single crystal, powder, and solution studies [1c].

In the present publication, we report the synthesis and X-ray structure analysis of a pair of isomeric Cu^{II} complexes of the tricyclic tetraamine ligands '*syn*'-L and '*anti*'-L (see *Scheme*; L = 1,4,8,10,13,15-hexaazatricyclo[13.3.1.1^{4,8}]icosane), and their solution-structure analysis with the MM-AOM approach. The complexes are obtained by a high-yielding Cu^{II}-directed condensation of 3,2,3-tet (= *N*,*N*''-(ethane-1,2-diyl)propane-1,3-diamine) with formaldehyde and ethane-1,2-diamine (= en; see *Scheme*) [2]. Similar products have been obtained by the corresponding Ni^{II}-directed condensation reaction [2a].

2. Results and Discussion. – 2.1. *Synthesis.* The Cu^{II}-directed condensation of 3,2,3-tet with formaldehyde and en leads in high yield (*ca.* 70%) to the tricyclic ligand L,

Scheme

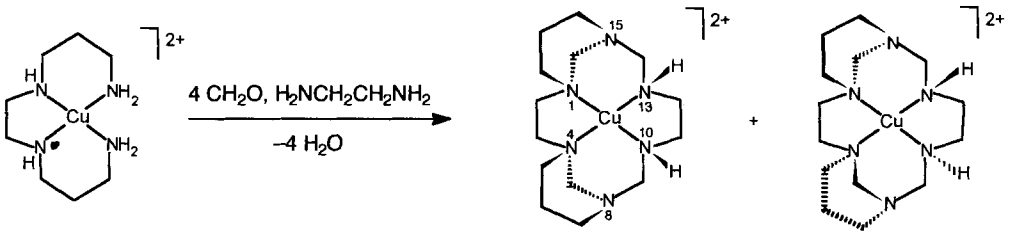

[Cu('*syn*'-L)]$^{2+}$ (*trans* I) + [Cu('*anti*'-L)]$^{2+}$ (*trans* IV)

coordinated to Cu^{II}, with a '*syn*'/'*anti*' ratio of *ca.* 1:2. The corresponding condensation reaction with dinitroalkanes instead of en as 'locking groups' [2b], and that using 2,3,2-tet as the tetraamine [3] fragment yield bismacrocyclic ligands as the main products. Probable reasons for the different reactivities are differences in the coordination equilibria involving the tetraamines and en (six- *vs.* five-membered chelate rings) and differences in the pK_a values and nucleophilicities of dinitroalkanes and amines. In an earlier report on $[Cu(L)]^{2+}$, the '*anti*' isomer was the only product [2a], and this is due to the different workup procedures, and possibly to an isomerization process similar to that observed in the corresponding Ni^{I}/Ni^{II} systems [4]. The separation of [Cu('*syn*'-L)]$^{2+}$ and [Cu('*anti*'-L)]$^{2+}$ was achieved by cation-exchange chromatography.

2.2. *Crystal Structure Analysis.* The two ligands, '*syn*'-L and '*anti*'-L, are derivatives of cyclam (1,4,8,11-tetraazacyclotetradecane), with the two central C-atoms of the propanediyl bridges (C(6) and C(13)) substituted by N-atoms, and with a propanediyl bridge *cis*-connected to each of these aminal moieties. These fix the configuration of the two coordinating tertiary-amine moieties, leading to the diastereoisomer pair of ligands with (1*R**,4*S**) ('*syn*') and (1*R**,4*R**) ('*anti*') configurations (for numbering, see *Scheme*). For metal complexes with cyclam-type ligands, five relative configurations with respect to the four amine donor atoms are possible with a planar coordination of the macrocyclic ligand, *i.e.*, (*R**,*S**,*R**,*S**), (*R**,*S**,*R**,*R**), (*R**,*S**,*S**,*R**), (*R**,*R**,*S**,*S**), and (*R**,*R**,*R**,*R**) (*trans* I–V) [5]. The conformations of the chelate rings are coupled to the configuration of the amine N-atoms and, since *gauche* (five-membered chelate rings) and chair conformations (six-membered chelate rings) are stabilized, the two diastereoisomers with (*R**,*R**,*S**,*S**) (*trans* IV) and (*R**,*S**,*R**,*S**) (*trans* I) configurations are favored. The former is the most stable form for complexes of the parent cyclam ligand, and for the tetra-*N*-methyl-substituted cyclam derivative, four-coordinate complexes have been found to be more stable in the (*R**,*S**,*R**,*S**) configuration, while five- and six-coordinate complexes prefer the (*R**,*R**,*S**,*S**) geometry [5].

The molecular cations of [Cu('*syn*'-L)]$(ClO_4)_2$ and [Cu('*anti*'-L)]$(ClO_4)_2 \cdot {}^1/_2\,H_2O$ are shown in *Fig. 1*; bond distances and valence angles of the two chromophores are given in *Table 1*. The configurations of the tertiary-amine N-atoms N(2) and N(3) (for numbering, see *Fig. 1*), fixed by the propanediyl bridges, are (*R**) and (*S**) for the '*syn*'- and (*R**) and (*R**) for the '*anti*'-isomer, respectively. The observed geometries are those expected from the enforced configurations at N(2) and N(3), and involving *gauche* and chair

conformations of the chelate rings, *i.e.* (*R**,*S**,*R**,*S**) (*trans* I) and (*R**,*R**,*S**,*S**) (*trans* IV) for the '*syn*'- and the '*anti*'-isomer, respectively. Ignoring the conformation of the five-membered chelate rings and those of the six-membered bridge rings, the idealized symmetries of the '*syn*'- and the '*anti*'-isomers are C_s and C_1 (C_2 if the axial ligand is neglected), respectively. Thus, with fluxional conformations, the '*syn*'-isomer is achiral (*meso*-form; (*R**,*S**,*R**,*S**,*R**,*S**) at N(2),N(3),N(4),N(1),N(6), and N(5), resp.), while the '*anti*'-isomer is chiral ((*R**,*R**,*S**,*S**,*S**,*S**) at N(2),N(3),N(4),N(1),N(6), and N(5), resp.). In the experimentally determined structures in the solid, all six-membered rings have chair conformations. The five-membered chelate rings of the '*syn*'-isomer both have λ conformations, while those of the '*anti*' isomer are λ and δ for the rings involving the tertiary- and the secondary-amines N-atoms, respectively.

In both isomers, a perchlorate O-atom completes the coordination sphere to yield distorted square-pyramidal geometries. For symmetry reasons (see above), there are in theory two identical axial sites for the '*anti*'-isomer. In the '*syn*'-isomer, the axial perchlorate is, as expected [6], disposed '*syn*' to the propanediyl bridges. The structural plot (*Fig. 1*) nicely shows the steric crowding on the opposite side of the N_4 plane, due to the methylene groups of the five-membered chelate rings. This interpretation is supported by the observed axial Cu–O bond distances, with a significantly shorter bond for the '*syn*'-isomer (2.463 *vs.* 2.571 Å), *i.e.*, some crowding due to the methylene groups is involved in the '*anti*'-isomer. In both structures, a second perchlorate O-atom is found at a Cu–O distance of over 3 Å. The Cu–N distances are as expected for [Cu^{II}(amine)] complexes, those of the '*anti*'-isomer being in average slightly but not significantly longer than those of the '*syn*'-isomer (2.034 *vs.* 2.027 Å; the average Cu–N distance of $[Cu(cyclam)]^{2+}$ is 2.020 Å [7]). In the angular geometry, there are considerable differences between the two isomers. While all bite angles are normal (*ca.* 93° for six-membered and *ca.* 87° for five-membered rings) and very similar for the two species, the angles involving the O-donor and the *trans*-disposed N-donors N(2) and N(4) indicate that, for the '*syn*'-isomer, there is a considerable distortion towards a trigonal bipyramidal coordination geometry, and thus reducing the idealized C_s symmetry to C_1.

2.3. *Spectroscopy.* The '*syn*'-isomer [Cu('*syn*'-L)]$(ClO_4)_2$ has a blue violet color in the solid and is blue in aqueous solution, while the '*anti*'-isomer [Cu('*anti*'-L)]-$(ClO_4)_2 \cdot {}^1/_2\, H_2O$ is red, both in the solid and in aqueous solution (*Fig. 2*, *Table 2*). The solution extinction coefficient of the '*syn*'-isomer ($\varepsilon_{600nm} = 205$ dm^3 mol^{-1}cm^{-1}) is significantly larger than that of the '*anti*'-isomer ($\varepsilon_{524nm} = 124$ dm^3 mol^{-1}cm^{-1}). Possible reasons for a shift of dd transitions of [Cu^{II}(tetraamine)] complexes to lower energy include an elongation of the Cu–N bonds, a strong interaction to axial ligands, and a distortion of the CuN_4 chromophore from planarity. The latter two features are evident from the solid-state structures, and the relatively high absorption intensity of the '*syn*'-isomer is consistent with the angular distortion of the chromophore (see above).

The spin-*Hamiltonian* parameters, resulting from the simulation of the frozen-solution EPR spectra, are also presented in *Table 2*. Relatively small hyperfine coupling constants and comparably large Δg values are a general observation for distorted [Cu^{II}(tetraamine)] complexes, and, based on simple ligand-field models, this may be traced back to decreasing ligand-field transition energies [1].

Thus, qualitatively, the experimental structures and the electronic and EPR spectra lead to a consistent picture of the system. However, based on these results alone, the color

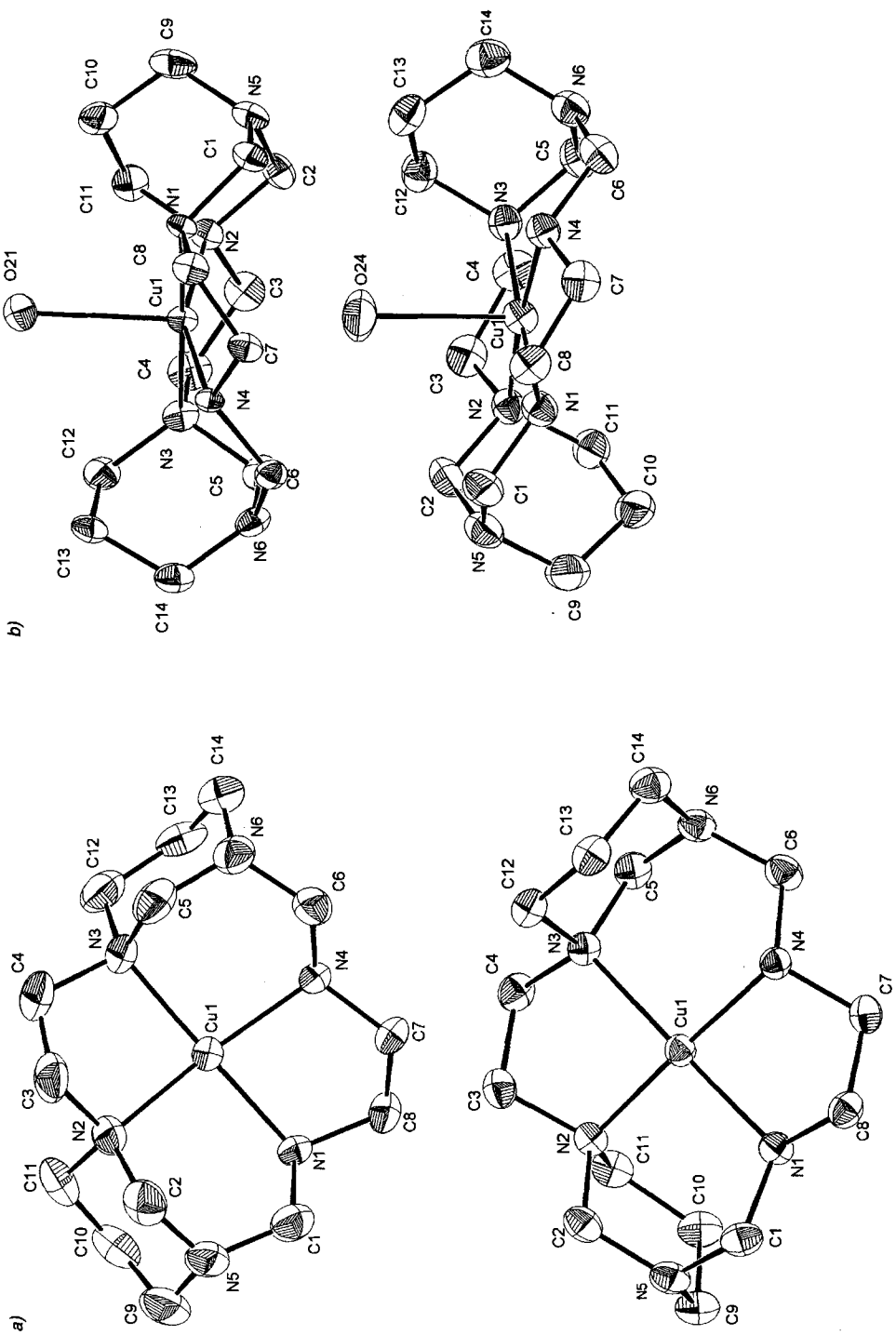

Fig. 1. *Experimentally determined structures of the molecular cations of* $[Cu(\text{'syn'-}L)](ClO_4)_2$ (top) *and* $[Cu(\text{'anti'-}L)](ClO_4)_2 \cdot {}^1/_2\ H_2O$. ORTEP Plots; *a*) top view without axial donors; *b*) side view without long-distance interaction to second axial ligand. Arbitrary numbering.

Table 1. *Observed Bond Distances and Valence Angles of the Chromophores of [Cu('syn'-L)](ClO$_4$)$_2$ and [Cu('anti'-L)](ClO$_4$)$_2$ · $^1/_2$ H$_2$O*[a]). Arbitrary numbering.

	[Cu('*syn*'-L)]$^{2+}$		[Cu('*anti*'-L)]$^{2+}$	
	exper.	calc.	exper.	calc.
Cu–N(1)	2.019(4)	2.075	2.031(3)	2.053
Cu–N(2)	2.038(4)	2.057	2.022(3)	2.067
Cu–N(3)	2.043(4)	2.078	2.067(3)	2.067
Cu–N(4)	2.008(4)	2.051	2.017(3)	2.053
Cu–O(21)[b])	2.463(4)	2.277[d])	2.571(3)	2.671[e])
Cu–O(13)	3.368(5)	–[d])	3.190(4)	2.671[e])
N(1)–Cu–N(2)	94.4(2)	95.5	92.6(1)	93.9
N(1)–Cu–N(3)	178.0(2)	177.5	178.3(1)	178.0
N(1)–Cu–N(4)	84.3(2)	83.5	85.5(1)	84.2
N(2)–Cu–N(3)	87.4(2)	86.7	88.0(1)	88.0
N(2)–Cu–N(4)	158.2(2)	152.0	175.3(1)	178.0
N(3)–Cu–N(4)	94.0(2)	95.0	93.8(1)	93.8
N(1)–Cu–O(21)[b])	90.8(1)	81.8	85.9(1)	86.2
N(2)–Cu–O(21)[b])	95.5(2)	105.6	97.7(1)	97.1
N(3)–Cu–O(21)[b])	88.0(2)	96.5	95.6(1)	92.9
N(4)–Cu–O(21)[b])	106.2(1)	101.8	86.4(1)	83.5
N(1)–Cu–O(13)[c])	86.5(1)	–[d])	78.1(1)	83.5
N(2)–Cu–O(13)[c])	84.7(1)	–[d])	94.8(1)	92.9
N(3)–Cu–O(13)[c])	94.7(2)	–[d])	99.5(1)	97.1
N(4)–Cu–O(13)[c])	73.9(1)	–[d])	80.7(1)	86.2

[a]) Also included are structural parameters for the computed molecular cations; note that these have axial H_2O molecules instead of ClO_4^-.
[b]) For '*anti*' O(24).
[c]) For '*anti*' O(11).
[d]) Five-coordinate.
[e]) Six-coordinate.

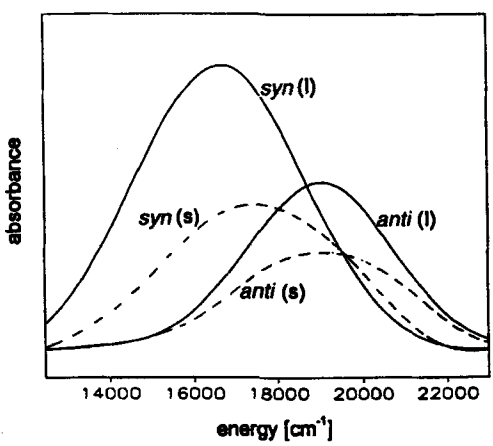

Fig. 2. *Electronic spectra of [Cu('syn'-L)](ClO$_4$)$_2$ and [Cu('anti'-L)](ClO$_4$)$_2$ · $^1/_2$ H$_2$O in the solid state* (s; ----) *and in solution* (l; ——)

Table 2. *Observed and Computed Spectroscopic Data*[a]) *of [Cu('syn'-L)](ClO$_4$)$_2$ and [Cu('anti'-L)](ClO$_4$)$_2$ · $^1/_2$ H$_2$O*

	[Cu('*syn*'-L)]$^{2+}$		[Cu('*anti*'-L)]$^{2+}$	
Solid state:	obs.[b])	AOM	obs.[b])	AOM
E_1	–	19800	–	20200
E_2	18400	19300	20000	20000
E_3	16300	17800	18400	19100
E_4	–	15300	–	15900
Solution:	obs.[b])	MM-AOM[d])	obs.[b])	MM-AOM[e])
E_1	–	17300	–	18900
E_2	17000	16800	19300	18800
E_3	15000	14700	18000	17900
E_4	–	12800	–	14100
EPR:	obs.[c])	MM-AOM[d])	obs.[c])	MM-AOM[e])
$g_\perp$	2.06	2.05, 2.05	2.04	2.04, 2.04
$g_\parallel$	2.21	2.18	2.20	2.17
$A_\perp$	49	13, 39	35	26, 29
$A_\parallel$	177	193	193	200

[a]) Electronic transitions in cm^{-1}; EPR hyperfine parameters in 10^{-4} cm^{-1}.
[b]) Based on *Gaussian* fits of the experimental spectra.
[c]) Based on simulated experimental spectra.
[d]) $\lambda\lambda$, five-coordinate.
[e]) $\lambda\delta$, six-coordinate.

change of the '*syn*'-isomer (solid *vs.* aqueous solution) is not explainable. An interpretation involving AOM calculations, based on the experimental and computed structures (MM-AOM), for the solid-state and solution spectra, respectively, requires an assignment of the electronic transitions. For the present study, we have based this on the assignment of a recently published thorough study, involving a large series of [Cu^{II}(tetraamine)] complexes with chromophores similar to those reported here, and involving single-crystal, powder, and solution UV/VIS-NIR and EPR spectroscopy [1c].

2.4. *Molecular-Mechanics Modeling.* The force-field calculations are based on a set of potential-energy functions that compute the angular geometry around the metal center with 1,3-nonbonded interactions [8]. The conformational analysis was based on 180 structures, *i.e.*, (*R**,*S**,*R**,*S**), (*R**,*S**,*R**,*R**), and (*R**,*S**,*S**,*R**) configurations (*trans* I–III) for the '*syn*'-isomer and (*R**,*R**,*S**,*S**) and (*R**,*R**,*R**,*R**) configuration (*trans* IV and V) for the '*anti*'-isomer, including four-, five-, and six-coordinate species (0, 1, or 2 axial OH_2 groups), δ- and λ-conformations of the five-membered chelate rings, and chair-chair, twist-twist, and boat-boat conformations of the six-membered bridge rings. The conformations of the six-membered chelate rings are rigid and coupled to the configurations of the secondary-amine groups. The structure optimization did not lead to any stable minima with a twist conformation of a six-membered bridge ring, reducing the number of strain energy minimized structures to 120. All structures with boat-boat

conformations were more strained by at least 10 kJ/mol, hence no mixed boat-chair conformations were considered.

As expected, the *trans* I ('*syn*'-isomer) and *trans* IV ('*anti*'-isomer) configurations, *i.e.*, those observed in the solid-state structures, were the most stable with a reasonable coordination geometry for a Cu^{II} complex. Some four-coordinate structures of relatively low energy were discarded due to a large tetrahedral twist of the CuN_4 plane, leading to calculated spectroscopic properties (MM-AOM, see below) in disagreement with the experimental data (the more general potential energy function set, using a metal-centered valence-angle function with a ligand-field-based force constant as a perturbation to the donor-donor-repulsion approach, developed for hexacoordinate transition-metal species [8b], is not well suited for square-planar compounds).

The strain energies of the lowest-energy conformations ('*syn*' = *trans* I; '*anti*' = *trans* IV) are listed in *Table 3* (four-, five-, and six-coordinate chromophores, δ and λ conformations of the five-membered chelate rings, chair conformations of the bridge six-membered rings). Note, that the conformations observed in the crystals are $\lambda\lambda$ and $\lambda\delta$ for the '*syn*'- and the '*anti*'-isomer, respectively (italicized in *Table 3*). For both isomers, this corresponds to the lowest-energy structures, irrespective of the coordination number. For the '*syn*'-isomer, the energy differences of *ca.* 10 kJ/mol to the corresponding $\lambda\delta$ conformers indicate that conformational changes are not a likely reason for the red-shift between the solid and the aqueous solution[1]). Note, that the classical molecular-mechanics analysis does not allow to assign the coordination number. However, the comparably low strain of the five-coordinate species is consistent with the relatively short bond to an axial perchlorate O-atom in the solid. Also, the saddle-shaped ligand geometry leads to a significant trigonal bipyramidal twist which is increased in the computed

Table 3. *Relative Strain Energies* [kJ/mol] *of All Relevant Computed Structures of [Cu("*syn*"-L)]$^{2+}$ and [Cu('*anti*'-L)]$^{2+}$*[a])[b])

	Coordination number	$\delta\delta$[c])	$\delta\lambda$[c])	$\lambda\delta$	$\lambda\lambda$
[Cu('*syn*'-L)]$^{2+}$	4			15	*6*
	5			11	*1*
	6			11	*4*
[Cu('*anti*'-L)]$^{2+}$	4	17	46	*7*	22
	5	16	45	*4*	21
	6	14	49	*0*	22

[a]) Six-membered chelate rings and bridge six-membered rings in chair-conformation.
[b]) Italicized values refer to conformations observed in the crystals.
[c]) For symmetry reasons, degenerate for the '*syn*'-isomer, see *Chapt. 2.2.*

[1]) Note that energy contributions due to entropic effects, ion pairing, and solvation are neglected in the molecular-mechanics calculations presented here. For a number of reasons, however, computations of this type may not be described as 'gas-phase calculations', and from similar studies it emerges that strain-energy differences of the size observed here (> 10 kJ mol^{-1}) are relevant as long as they are compared to relevant experimental data obtained in identical reaction media (*i.e.*, dilute aqueous solutions of the perchlorate salts in the present example) [1c] [9].

structure of the five-coordinate species (N(2)–Cu–N(4): 158.0° *vs.* 152.0°), and this is supported by the spectral changes (see ahead). For the $\lambda\delta$ conformation of the '*anti*'-isomer, the strain energy decreases significantly with an increasing coordination number. From the C_2 symmetry of the Cu('*anti*'-L) fragment, a four- or six-coordinate compound was expected in solution. Due to the considerably smaller strain energy of the six-coordinate species, the MM-AOM analysis (see below) was based on this geometry.

2.5. *AOM Calculations.* The AOM calculations were done as those of an earlier study, using a constant set of copper-donor distance dependent e_σ and e_π values and $e_{ds} = {}^1/_4\, e_\sigma$ [1c]. Parameters not defined before are given in the *Exper. Part.* The computed electronic transitions are listed together with the experimental data in *Table 2.* The assignment of the transitions is based on low-temperature single-crystal work of similar chromophores [1c]. It is not unexpected that the nearly degenerate transitions, involving the d_{xz} and d_{yz} orbitals, and the low-energy transition, involving the d_{z^2} orbital, are not resolved in the room-temperature spectra discussed here. The transitions, computed on the basis of the experimental structural data, are in acceptable agreement with the two transitions each observed in the solid-state spectra.

From the AOM analysis of the '*syn*'-isomer, based on the computed structures of all relevant conformers (see *Table 3*), it followed that only for the $\lambda\lambda$ conformation of the five-coordinate chromophore there is good agreement between the computed transitions and those observed in the solution electronic spectrum. The calculated energy levels of all other low-strain structures are at least 1500 cm^{-1} higher than the observed absorptions. For the '*anti*'-isomer, the calculated transitions of computed structures with $\lambda\delta$ conformations lead to acceptable agreement with the corresponding solution spectrum. However, each of the two relevant calculated transitions (E_2 and E_3 in *Table 2*) are roughly independent ($\pm$ 500 cm^{-1}) of the coordination number (four-, five-, or six-coordinate chromophores; the data presented are for the six-coordinate species). Therefore, based on the spectroscopic properties, it is not possible to determine the coordination number of the '*anti*'-isomer.

The *g* values, obtained by AOM calculations, based on the computed structures, and the hyperfine parameters, computed as described previously [1c], are also compared to the experimental data in *Table 2.* The accuracy of the spin-*Hamiltonian* parameters is acceptable but lower than expected on the basis of previous studies [1c] and the quality of the computed electronic transitions, especially for the '*syn*'-isomer. A probable reason is the highly flexible and possibly medium-dependent geometry of the '*syn*'-isomer, coupled with the fact that, for the EPR spectra, a different temperature was used. However, the general trend, *i.e.*, a more extensive distortion from planarity of the CuN_4 chromophore and a stronger interaction to the axial O-donor for the '*syn*'-isomer compared to the '*anti*'-isomer, leading to lower-energy electronic transitions and consequently to larger Δg and smaller $A_\parallel$ values, is in agreement with the observed and computed spectroscopic data. The solution-structure parameters, based on the MM and MM-AOM calculations, appear in the table of the observed solid-state structural data (*Table 1*; note, that the axial donors for the solution structures are OH_2 instead of ClO_4^-, thus the disagreement between observed and computed Cu–L distances is not unexpected, see also *Chapt. 1.*

Model AOM calculations, involving distortions along three relevant modes, were also used to analyze the spectroscopic differences of the '*syn*'-isomer in the solid state and

in solution. The model calculations include: *i*) elongation of the axial Cu–O distance, *ii*) simultaneous elongation of the four Cu–N bonds, and *iii*) compression of the N(2)–Cu–N(4) angle. A combination of *i*) and *ii*) corresponds to a *Jahn-Teller* distortion, while *iii*) is related to a *Berry* twist, and both of these distortion modes have been shown to be of importance in the present examples. For the model calculations along the *Berry*-twist coordinate, the N(2)–Cu–N(4) angle was varied between 140 and 180°, while all other internal coordinates were constrained at the X-ray structure positions (*Fig. 3a*). To visualize the influence of the variation in copper-donor distances on the electronic transitions, the transition energy (E_2) is plotted in *Fig. 3b* as a function of the variation of the averaged equatorial bond lengths, coupled with a simultaneous compression of the axial bond (inverse correlation of the equatorial and the axial bond distance [10]). The model calculations indicate that in the range covered by the '*syn*'-isomer (152° < N(2)–Cu–N(4) < 158°, and 2.027 Å < Cu–N_{av} < 2.065 Å; MM *vs.* X-ray, see *Table 1*), the dependence of the transition energy from the two distortion modes is roughly linear, and the variation due to the radial distortion is more pronounced than

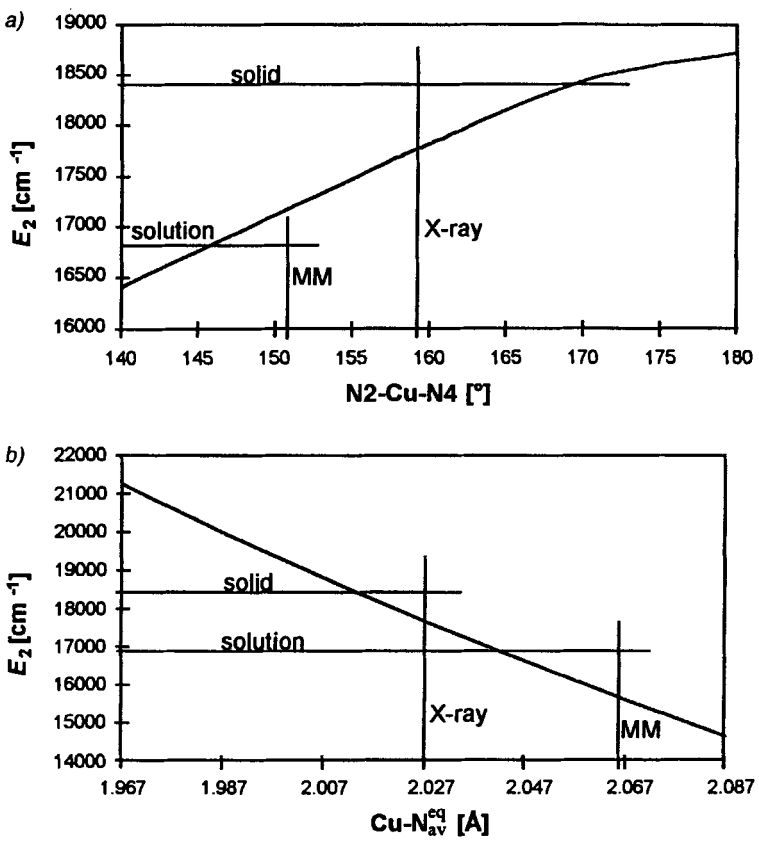

Fig. 3. *Model AOM calculations of the* E_2 *transition, involving,* a) *a* Berry-*twist distortion and* b) *a* Jahn-Teller *distortion* (see text). Also included are the observed and computed structural (vertical lines) and spectroscopic (horizontal lines) values.

that based on the angular distortion. It also emerges that the higher energy of the transitions in the '*anti*'-isomer, with slightly expanded Cu–N distances, indicate a roughly planar chromophore.

3. Conclusions. – The experimentally determined solid-state structures of the two isomeric [Cu^{II}(tetraamine)] complexes, [Cu('*syn*'-L)]$(ClO_4)_2$ and [Cu('*anti*'-L)](ClO_4) · 1/2 H_2O, have the expected configurations, *viz. trans* I and *trans* IV, respectively. This is supported by the calculated strain energies. Moreover, the experimentally observed chelate-ring conformations are more stable than any other conformation by at least 10 kJ/mol[1]). Due to the geometry of the '*syn*'-ligand, one axial site is partially shielded, leading to a five-coordinate, distorted square-pyramidal chromophore. This is supported by the molecularmechanics analysis and the spectroscopic results. For the '*anti*'-isomer, a six-coordinate structure might have been expected. The experimentally observed five-coordinate structure probably is due to the arrangement of the molecular cations in the crystal lattice, and the solution structure most likely is six-coordinate. This is consistent with all the data presented, but a four- or five-coordinate structure may not be excluded with certainty. The striking spectroscopic difference between the two isomers can be attributed to an angular distortion along a *Berry*-twist coordinate. The MM-AOM calculations suggest that the color change of the '*syn*'-isomer upon dissolution in H_2O (red shift of *ca.* 1500 cm^{-1}) is due to an increasing distortion along the *Berry*-twist coordinate, coupled with bond-length changes. A change of the coordination number, of the configuration of the coordinated N-donors, or of the chelate-ring conformations is improbable. Thus, in this case, the differences between solid-state and solution properties may be traced back to some strain imposed by the crystal lattice. The fact that the MM-AOM calculations lead to a good agreement between the observed and computed spectroscopic properties indicates that the forces to keep the CuN_4 chromophore planar are, as expected, rather weak. Thus, the approach to compute the angular geometry of [Cu^{II}(tetraamine)] complexes with 1,3-nonbonded interactions alone is reasonable [8b].

Experimental Part

Caution: Perchlorate salts are potentially explosive and should be handled with care.

1. *General.* $Cu(ClO_4)_2 \cdot 6\,H_2O$, 3,2,3-tet (*N,N''*-(ethane-1,2-diyl)propane-1,3-diamine) and en (ethane-1,2-diamine) were obtained from *Aldrich*. [Cu(3,2,3-tet)]$(ClO_4)_2$ was prepared by reaction of $Cu(ClO_4)_2 \cdot 6\,H_2O$ with stoichiometric amounts of 3,2,3-tet in MeOH. Partial evaporation of the solvent under reduced pressure yielded the product as a crystalline solid. UV/VIS Spectra: *Varian-Cary-2300* and *Varian-Cary-1E* spectrophotometer for powder and soln. spectra; the experimental spectra were fitted with four *Gaussian* curves; only the maxima of the major contributors are listed in *Table 2*. IR Spectra (KBr pellets): *Perkin-Elmer-16PC* FT-IR instrument; $\tilde{\nu}$ in cm^{-1}. EPR Spectra: 10^{-3} mol/l in DMF/H_2O 1:2, frozen soln. at 120 K; *Bruker-ESP-300E* instrument; the spin-*Hamiltonian* parameters were determined by simulation of the experimental spectra with the computer program EPR50F [11]. Elemental analyses were obtained from the Microanalytical Laboratory of the Chemical Institutes of the University of Heidelberg.

2. *Synthesis.* To a soln. of [Cu(3,2,3-tet)]$(ClO_4)_2$ (2.0 g, 4.8 mmol) in MeOH/H_2O 4:1 (25 ml) were added en (0.28 g, 4.8 mmol) and 38% aq. formaldehyde soln. (2.2 ml, 26.6 mmol). The soln. was refluxed for 24 h, diluted with H_2O to 1000 ml, and adsorbed onto a column of cation-exchange resin (*SP Sephadex C25*, Na^+ form, 3 × 40 cm). Elution with aq. $NaClO_4$ soln. (0.15 mol/l) separated a blue and a red fraction. Within several days at r.t., the fractions deposited blue crystals of [Cu('*syn*'-L)]$(ClO_4)_2$ and red crystals of [Cu('*anti*'-L)]$(ClO_4)_2 \cdot$ 1/2 H_2O, both suitable for crystal-structure studies. IR: 3261, 3266 (NH) for both isomers. UV/VIS and EPR: *Table 2*.

*[Cu('*syn*'-L)](ClO$_4$)$_2$*: 0.65 g (25.5%). Anal. calc. for $C_{14}H_{30}Cl_6CuN_6O_8$: C 30.86, H 5.55, N 15.42; found: C 30.54, H 5.35, N 15.42.

[Cu('anti'-L)](ClO$_4$)$_2$ · 1/2 H$_2$O: 1.15 g (43.6%). Anal. calc. for $C_{14}H_{32}Cl_6CuN_6O_{8.5}$: C 30.36, H 5.64, N 15.17; found: C 30.90, H 5.42, N 15.52.

3. *Crystal-Structure Analyses.* The atom numbering is given in *Fig. 1*. The crystallographic data have been deposited at the *Cambridge Crystallographic Data Centre (CCDC)*.

[(1S,4R*,8S*,10S*,13R*,15R*)-1,4,8,10,13,15-Hexaazatricyclo[13.3.1.1^{4,8}]icosan-κ^{4}N^1,N^4,N^{10},N^{13}]-copper*(II) *Diperchlorate* ([Cu('*syn*'-L)](ClO$_4$)$_2$): Mol. mass ($C_{14}H_{30}Cl_2CuN_6O_8$) 544.88; violet parallelepipeds (crystal dimensions 0.35 · 0.40 · 0.50 mm^3), monoclinic space group $P2_1/n$; a = 7.835(4), b = 14.259(9), c = 19.103(8) Å; β = 93.40(4)°; V = 2130.4 Å; Z = 4; $\rho_{calc.}$ = 1.70 gcm^{-3}; $F(000)$ = 1132; μ = 1.33 mm^{-1}; min./max. transmission 0.82–1.00; 3934 reflections were measured at r.t. on a *Nicolet-R3* diffractometer, employing graphite monochromated MoK_α radiation (λ = 0.7107 Å); ω scan mode; data reduction and application of *Lorentz* and polarization absorption corrections were carried out. Empirical absorption correction was carried out. The structure was solved by *Patterson-Fourier* methods with the SHELXTL PLUS program [12]; H-atoms were included at calculated sites with fixed isotropic thermal parameters. The refinement (full-matrix, least-squares methods, $|F|$ of 281 variables out of 2556 reflections with $I > 2.5\sigma(I)$ converged at R = 5.3% and R_w = 4.3%; residual electron density 0.48–0.43 eÅ^{-3}. Weight = $1/\sigma^2(F)$; goodness of fit = 1.73.

[(1R,4R*,8S*,10S*,13S*,15S*)-1,4,8,10,13,15-Hexaazatricyclo[13.3.1.1^{4,8}]icosan-κ^{4}N^1,N^4,N^{10},N^{13}]-copper(II) Dichlorate Hemitryobate* ([Cu('*anti*'-L)](ClO$_4$)$_2$ · 1/2 H$_2$O): The structure was solved as indicated above. Relevant parameters are: Mol. mass ($C_{14}H_{31}Cl_2CuN_6O_{8.5}$) 553.89; red prisms (crystal dimensions 0.61 · 0.65 · 0.72 mm^3), monoclinic space group $C2/c$; a = 32.74(2), b = 9.438(4), c = 14.803(7) Å; β = 110.36(4)°; V = 4288.4 Å^3; Z = 8; $\rho_{calc.}$ = 1.72 g cm^{-3}; $F(000)$ = 2304; μ = 1.33 mm^{-1}; min./max. transmission 0.75–1.00; 6123 reflections. The refinement (full-matrix, least-squares methods, $|F|$) of 286 variables out of 4104 reflections with $I > 2.5\sigma(I)$ converged at R = 4.3% and R_w = 3.5%; residual electron density 0.55–0.53 eÅ^{-3}. Weight = $1/\sigma^2(F)$; goodness of fit = 3.07.

4. *Calculations.* For MM calculations, we used MOMEC [13]. The force field used has been described previously [8]. AOM Calculations were performed with a modified version of CAMMAG [14], and the parameters used were described previously [1c]. The e_σ values for tertiary amines (C = 492470, $e_\sigma = C/r^6$, r = Cu–N) were determined by a linear extrapolation of primary and secondary amines. The parametrization of other metal-amine interactions (Cr^{III}–N, Co^{III}–N, Ni^{II}–N) indicates that this is a reasonable approach [1]. We also used a transferable parameter set for axially coordinated O-donors (C = 230000). The C-value for O-donors was determined by a minimization of the r.m.s. deviation of a r^{-6} function from a published plot fur Cu–O from 2.2 to 2.8 Å [15].

We are grateful for financial support by the *German Science Foundation (DFG)*.

REFERENCES

[1] a) P. V. Bernhardt, P. Comba, *Inorg. Chem.* **1993**, *32*, 2798; b) P. Comba, *ibid.* **1994**, *33*, 4577; c) P. Comba, T. W. Hambley, M. A. Hitchman, H. Stratemeier, *ibid.* **1995**, *34*, 3903; d) P. Comba, *Comments Inorg. Chem.* **1994**, *16*, 133.

[2] a) M. P. Suh, S.-G. Kang, V. L. Goedken, S.-H. Park, *Inorg. Chem.* **1991**, *30*, 365; b) P. Comba, P. Hillenhaus, *J. Chem. Soc., Dalton Trans.* **1995**, 3269.

[3] S. V. Rosokha, Y. D. Lampeka, I. M. Maloshtan, *J. Chem. Soc., Dalton Trans.* **1993**, 631; D. Lee, M. P. Suh, J. W. Lee, *ibid.* **1997**, 577.

[4] M. P. Suh, K. Y. Oh, J. W. Lee, Y. Bae, *J. Am. Chem. Soc.* **1996**, *118*, 777.

[5] B. Bosnich, C. K. Poon, M. L. Tobe, *Inorg. Chem.* **1965**, *4*, 1102.

[6] T. W. Hambley, *J. Chem. Soc., Dalton Trans.* **1986**, 565.

[7] P. A. Tasker, L. Sklar, *J. Cryst. Mol. Struct.* **1975**, *5*, 329.

[8] a) P. V. Bernhardt, P. Comba, *Inorg. Chem.* **1992**, *31*, 2638; b) P. Comba, T. W. Hambley, M. Ströhle, *Helv. Chim. Acta* **1995**, *78*, 2042.

[9] P. Comba, T. W. Hambley, 'Molecular Modeling of Inorganic Compounds', VCH, Weinheim, 1995; P. Comba, *Coord. Chem. Rev.* **1993**, *123*, 1; P. Comba, in Fundamental Principles of Molecular Modeling, Eds. W. Gans, A. Amann, and J. C. A. Boeyens, Plenum Press, New York, 1996, p. 167.

[10] J. Gazo, I. B. Bersuker, J. Garaj, M. Kabesová, J. Kohout, H. Langfelderova, M. Melni, M. Serátor, F. Valach, *Coord. Chem. Rev.* **1976**, *19*, 253; B. J. Hathaway, P. G. Hodgson, *Inorg. Nucl. Chem.* **1973**, *35*, 4071.

[11] P. A. Martinelli, G. R. Hanson, J. S. Thompson, B. Holmquist, J. R. Pilbrow, B. L. Vallee, *Biochemistry* **1980**, *28*, 225.

[12] G. M. Sheldrick, SHELXTL PLUS, Release 4.11 (V), Universität Göttingen, 1990.
[13] P. Comba, T. W. Hambley, G. Lauer, N. Okon, 'MOMEC, a Molecular Mechanics Program for Inorganic Compounds', Lauer & Okon, Heidelberg, Germany, e-mail: CVS-HD@T-ONLINE.DE, 1997.
[14] M. Gerloch, 'CAMMAG, a Fortran Program for AOM Calculation', University of Cambridge, UK; H. Stratemeier, M. A. Hitchman, P. Comba, P. V. Bernhardt, M. Riley, *Inorg. Chem.* **1991**, *30*, 4088.
[15] D. W. Smith, *Struct. Bond.* **1972**, *12*, 50.